Engineering Notes

ENGINEERING NOTES are short manuscripts describing new developments or important results of a preliminary nature. These Notes cannot exceed 6 manuscript pages and 3 figures; a page of text may be substituted for a figure and vice versa. After informal review by the editors, they may be published within a few months of the date of receipt. Style requirements are the same as for regular contributions (see inside back cover).

Investigation of the Nonlinear Flight Dynamics of Ordnance Weapons

JOHN D. NICOLAIDES,* CHARLES W. INGRAM,† AND THOMAS A. CLARE‡
University of Notre Dame, Notre Dame, Ind.

Nomenclature

A	=	reference area $\pi d^2/4$, ft^2
$C_{M\alpha}$	=	pitching moment stability coefficient $M\alpha/(QAd)$, rad^{-1}
$C_{Mq} + C_{M\dot{\alpha}}$	=	damping moment stability coefficient $(M_q + M_{\dot{\alpha}})/(QAd^2/2V)$, rad^{-1}
$C_{Mp\alpha}$	=	Magnus moment stability coefficient $M_{p\alpha}/(QAd^2/2V)$, rad^{-2}
d	=	reference length, ft
M_0	=	Mach number
Q	=	dynamic pressure, lb/ft^2
V	=	velocity, fps
α	=	angle of attack, deg
$\|\alpha\|$	=	magnitude of the complex angle of attack, deg

Introduction

VARIOUS weapon systems have experienced serious flight instabilities causing large wobbling motions and consequent inaccuracies. Since observed flight instabilities are not readily explainable by the linear aeroballistic theory,[1] it is necessary to employ nonlinear techniques.[2,3] Dynamic wind tunnel tests were conducted in order to establish the nonlinearities of the aerodynamic stability coefficients. The various types of tests and configurations covered in this investigation are as follows: 1) one-degree-of-freedom (1-D) free oscillation tests of the Snakeye Bomb in the transonic facility of the U.S. Naval Ship Research and Development Center (NSRDC), 2) 1-D test of the Low-Drag Bomb in the subsonic wind-tunnel at the Univ. of Notre Dame, 3) three-degree-of-freedom tests[4] of the 2.75 in. Folding Fin Aircraft Rocket (FFAR) in the Notre Dame subsonic tunnel, 4) supersonic free-flight wind-tunnel tests of the 2.75 in. FFAR in the Jet Propulsion Laboratory facility, and 5) full-scale free-flight tests of the Split-Skirt Bomb by the Weapons Research Establishment of Australia.[5]

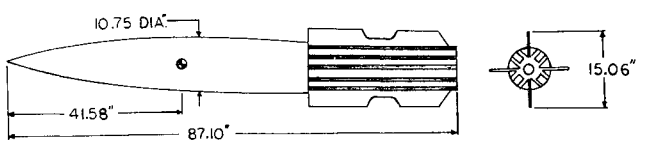

Fig. 1 The snakeye bomb.

Presented as Paper 69-135 at the AIAA 7th Aerospace Sciences Meeting, New York, January 20–22, 1969; submitted February 11, 1969; revision received July 6, 1970.

* Professor, Aerospace and Mechanical Engineering Department. Associate Fellow AIAA.

† Assistant Professor, Aerospace and Mechanical Engineering Department. Member AIAA.

‡ Research Assistant, Aerospace and Mechanical Engineering Department. Member AIAA.

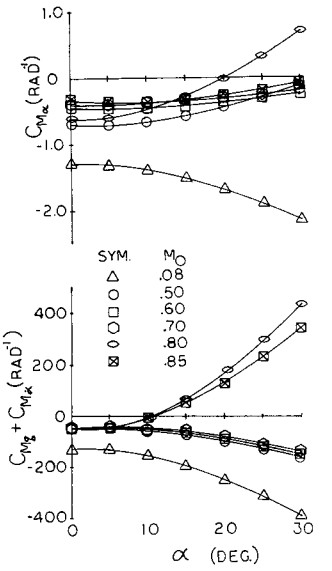

Fig. 2 Restoring and damping moment stability coefficients for the snakeye bomb.

In order to determine the nonlinear aerodynamic stability coefficients for these configurations, the theory of Ref. 3 was fitted to the missile's angular motion, using the "Wobble" computer program.[6] This program fits the epicyclic theory to overlapping sections of angular data. In this manner, the angle of attack variations of the restoring, damping, and Magnus moment coefficients can be obtained from a single set of experimental data. The nonlinear variation of the coefficients was specified as a polynomial function of the magnitude of the angle of attack in the following manner: 1) the restoring moment, $C_{m\alpha}(|\alpha|) = C_{m\alpha_0} + C_{m\alpha_2}|\alpha|^2$, 2) the damping moment, $(C_{mq} + C_{m\dot{\alpha}})(|\alpha|) = (C_{mq} + C_{m\dot{\alpha}})_0 + (C_{mq} + C_{m\dot{\alpha}})_2|\alpha|^2$, and 3) the Magnus moment, $C_{mp\alpha}(|\alpha|) = C_{mp\alpha} + C_{mp\alpha_2}|\alpha|^2$.

Wind-Tunnel Results

Transonic wind-tunnel tests were conducted on the unretarded Snakeye Bomb (Fig. 1) at the NSRDC employing a 1-D free oscillation technique. Figure 2 shows the computed variations of restoring moment and damping moment coefficients. It is apparent that these stability coefficients are nonlinear in α and that static and dynamic instabilities may occur at increasing values of M_0 and α. In addition, it was observed during the tests that, at $M_0 = 0.85$, normal shocks formed on the fins, causing static instability to occur at low α. It is recommended that further investigations be conducted to examine the possibility of eliminating this shock-fin interaction.

1-D free oscillation tests were conducted in the subsonic wind tunnel at Notre Dame on the Low-Drag Bomb with

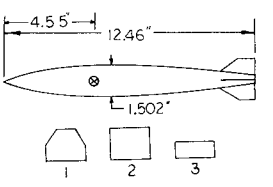

Fig. 3 Model and fin configurations of the low-drag bomb ($M_0 = 0.1$).

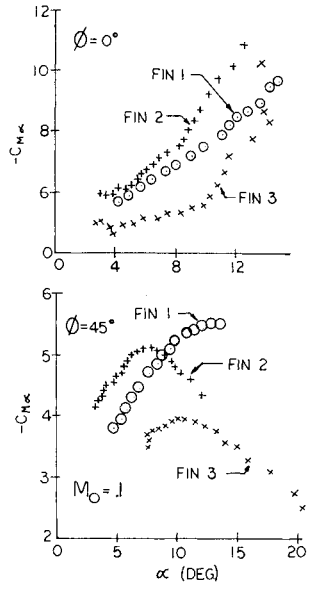

Fig. 4 Restoring moment stability coefficient for the low-drag bomb.

three different fin configurations (Fig. 3). It should be noted that all three fin configurations have the same span. Figures 4 and 5 show $C_{m\alpha}$ and $C_{mq} + C_{m\dot{\alpha}}$, respectively, as functions of α for roll orientations ϕ of 0° and 45°. For both ϕ's the degree of static stability varies inversely to the aspect ratio for the fin configurations tested. Static stability is greater at $\phi = 0°$ than at $\phi = 45°$ for all fin configurations. Figure 6 indicates that damping stability is also better at $\phi = 0°$.

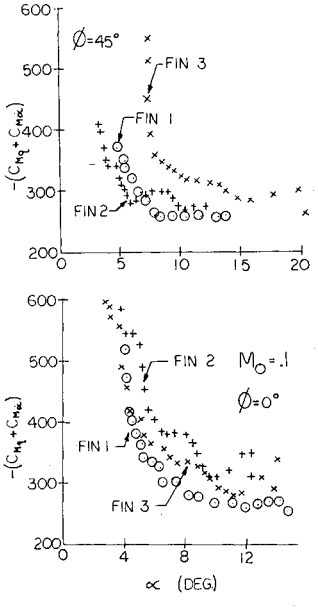

Fig. 5 Damping moment stability coefficient for the low-drag bomb (M_0 = 0.1).

Three-degree-of-freedom (pitch, yaw, and roll) wind-tunnel tests were conducted on the 2.75 in. FFAR in the subsonic tunnel at Notre Dame. These tests utilized a jewel bearing support system which minimizes the nonaerodynamic friction. This model (Fig. 6) had a wrap-around three finned tail assembly.

The model exhibited a precession limit cycle at $|\alpha| \simeq 2°$. At $|\alpha| > 20°$, however, a nutation limit cycle was observed.

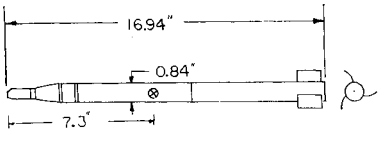

Fig. 6 Wind-tunnel model of the 2.75 in. FFAR.

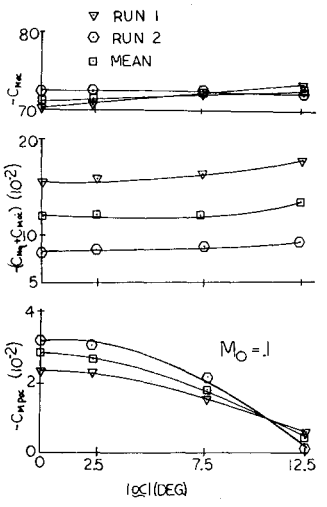

Fig. 7 Restoring, damping, and magnus moment stability coefficients for the 2.75 in. FFAR from 3-D wind-tunnel tests (M_0 = 0.1).

In order to obtain quantitative results, angular motions were analyzed for $3° < |\alpha| < 18°$. $C_{m\alpha}(|\alpha|)$, $(C_{mq} + C_{m\dot{\alpha}})(|\alpha|)$ and $C_{mp\alpha}(|\alpha|)$ are presented in Fig. 7. The restoring and damping moments are essentially insensitive to $|\alpha|$, but the Magnus moment exhibits a strong nonlinear variation with $|\alpha|$, indicating the possibility of a precession instability at low $|\alpha|$ and a nutation instability at $|\alpha| > 13°$ for the full-scale configuration. These results agree with the dynamic behavior of the 2.75 in. FFAR observed in the wind-tunnel tests.

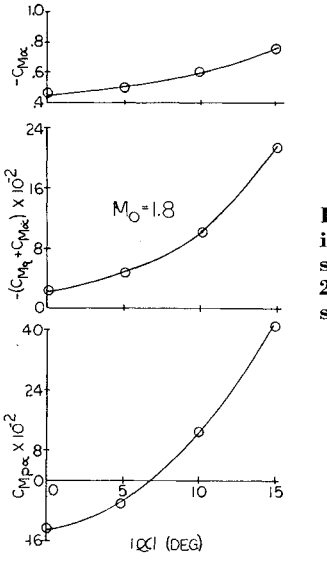

Fig. 8 Restoring, damping, and magnus-moment stability coefficients for 2.75 in. FFAR from supersonic free-flight wind-tunnel tests (M_0 = 1.8).

Free-flight wind-tunnel tests of the 2.75 in. FFAR with a cruciform curved fin configuration were conducted at the Jet Propulsion Laboratory (JPL). $C_{m\alpha}$, $C_{mq} + C_{m\dot{\alpha}}$, and $C_{mp\alpha}$ vs $|\alpha|$ are shown in Fig. 8. It is seen that $C_{mp\alpha}$ changes sign from negative to positive at $|\alpha| \simeq 8°$. These data indicate the possibility of a precession instability at low $|\alpha|$ and a nutation instability at larger $|\alpha|$. These trends are consistent with the results obtained from the aforementioned subsonic tests.

Full scale drop tests of the Split-Skirt Bomb (Fig. 9) were conducted at the Woomera Test Range, Salisbury, Australia. Values of $C_{m\alpha}$, $C_{mq} + C_{m\dot{\alpha}}$ and $C_{mp\alpha}$ at $|\alpha| = 7°$ and 12° as obtained from the "Wobble" analysis of the angular motion are

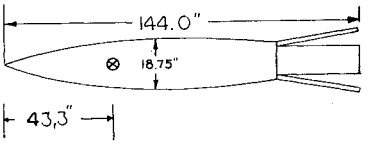

Fig. 9 The split-skirt bomb.

Table 1 Restoring, damping and magnus moment stability coefficients for the split-skirt bomb from free-flight tests

$\lvert\alpha\rvert$	C_{m_α} (rad^{-1})	$C_{m_q} + C_{m_{\dot\alpha}}$ (rad^{-1})	C_{mp_α} (rad^{-2})
7°	−0.7	−49.0	15.0
12°	−2.8	−49.0	18.0

given in Table 1. As seen from these data, the restoring and Magnus moment are nonlinear with $|\alpha|$, while the damping remained constant.

Conclusion

This investigation has shown that the restoring, damping, and Magnus moments must be considered as nonlinear functions of angle of attack for those configurations tested. It is evident, from these tests, that in order to accurately predict dynamic stability of ordnance weapons, the nonlinear variations of the aerodynamic stability coefficients must be accounted for. Furthermore, this study has demonstrated the requirement for additional dynamic testing and nonlinear evaluations of dynamic stability of current and future ordnance weapons designs.

References

[1] Nicolaides, J. D., *Free Flight Dynamics*, Univ. of Notre Dame, Notre Dame, Ind., 1961, pp. 103–204.

[2] Murphy, C. H., "Free Flight Motion of Symmetric Missiles," BRL Rept. 1216, 1963, Aberdeen Proving Ground, Md.

[3] Ingram, C. W., "On Obtaining the Nonlinear Aerodynamic Stability Coefficients from the Free Angular Motion of a Rigid Body," Ph.D. thesis, June 1969, Univ. of Notre Dame, Notre Dame, Ind.

[4] Nicolaides, J. D. et al., "Nonlinear Aerodynamic Stability Characteristics of the 2.75 in. Wrap-Around Fin Configuration," Paper 31, *Proceedings of the 8th Navy Symposium on Aeroballistics*, Vol. 3, May 1969.

[5] Clare, T. A., "An Investigation of the Dynamic Behavior of a Split-Skirt Bomb in Free-Flight," AFATL-TR-69-109, Aug. 1969, Elgin Air Force Base, Fla.

[6] Eikenberry, R. S., "Analysis of the Angular Motion of Missiles," SC-CR-70-6051, Feb. 1970, Sandia Labs., Albuquerque, N. Mex.

Methods for Computing Effects of Secondary Fluid Injection on Rocket Engine Performance

R. R. Stromsta* and G. A. Hosack†
Rocketdyne, North American Rockwell Corporation, Canoga Park, Calif.

Nomenclature

A_t = geometric throat area
A^* = effective throat area, A_tC_D
B,C = constants in aerobell theory
c^* = characteristic velocity, $P_cA^*g_c/\dot w$
C_D = discharge coefficient at throat, $\dot w_{\text{actual}}/\dot w_{\text{ideal}}$
C_F = nozzle vacuum thrust coefficient, F/P_oA^*
$C_{F(\text{id},\epsilon^*)}$ = ideal C_F at a specified ϵ^* and γ
$C_F{}^*$ = ideal C_F at sonic conditions, F^*/P_oA^*
$C_{F_{p(\text{inv})}}$ = inviscid C_F of primary nozzle
F = nozzle axial thrust (vacuum conditions)
g_c = gravitational units conversion factor
I = vacuum specific impulse, $F/\dot w$, c^*C_F/g_c
K_1,K_2,K_3 = constants in aerobell theory
MW = molecular weight
P,P_w = pressure and wall static pressure
$P_{os}{}^*$ = effective stagnation pressure of secondary flow
R = universal gas constant
R_t = throat radius
T = temperature
$\dot w$ = weight flowrate
β = oblique shock angle (Fig. 2)
γ = specific heat ratio
δ = loss factor relative to ideal expansion
ϵ^* = effective area ratio, A_e/A^*
$\epsilon_i{}^*$ = effective area ratio at secondary injection location, $A_i/A_p{}^*$
$\epsilon_0{}^*$ = effective overall area ratio of aerobell, $A_e/A_p{}^*$
ϵ'_p = area ratio of primary flow after being displaced by the secondary flow, $A'_{p_e}/A_p{}^*$
η_F = nozzle vacuum thrust efficiency, $C_F/C_{F(\text{id},\epsilon^*)}$
θ = flow angle downstream of oblique shock relative to upstream flow (Fig. 2)
θ_e = nozzle wall angle at exit plane
ξ = $\dot w_sc_s{}^*/\dot w_pc_p{}^*$; ξ_0 = value at Region 1–2 interface

Superscripts

* = sonic conditions
′ = properties of flow displaced by secondary flow

Subscripts

1,2 = upstream and downstream of oblique shock, respectively
B,c,E = base, chamber (primary), and engine, respectively
e,i = exit and injection conditions, respectively
o,p,s = stagnation, primary, and secondary, respectively
t,w = throat and wall, respectively

Introduction

THIS Note presents simple analytical and semiempirical methods for determining the effects of secondary flow injection on engine performance. Three methods of secondary flow injection into bell nozzles are considered: subsonic flow through a porous mesh or slots in the expansion nozzle walls, supersonic tangential secondary injection through an annular nozzle, and subsonic injection into the base region of an aerobell nozzle using a downstream facing step discontinuity (Fig. 1). The results are compared with cold-flow and simulated hot-flow experimental data. Details on the aerobell nozzle concept and the models tested have been previously reported.[1,2]

Theoretical Models

For systems utilizing secondary flow, the vacuum thrust coefficient and the engine vacuum specific impulse are

$$C_F = Fg_c/(\dot w_pc_p{}^* + \dot w_sc_s{}^*) \quad (1)$$

$$I_E = F/(\dot w_p + \dot w_s) \quad (2)$$

A required input is the vacuum thrust performance in the absence of secondary flow. For nozzles with continuous or nearly continuous wall contours (Figs. 1a and 1b), the method of characteristics is used to compute the inviscid flowfield between the throat and the exit plane assuming shifting equilibrium flow. The resulting $C_{F_{p(\text{inv})}}$ is compared with the ideal one-dimensional value based on the effective area ratio $\epsilon_p{}^*$ to compute the divergence loss, $\delta_{\text{div}} = 1 - C_{F_{p(\text{inv})}}/C_{F_{p(\text{id},\,\epsilon_p{}^*)}}$. A solution for the boundary layer yields the friction drag loss, $\delta_{\text{drag}} = \Delta C_{F(\text{drag})}/C_{F_{p(\text{id},\,\epsilon_p{}^*)}}$. Similarly, we

Presented as Paper 69-473 at the AIAA 5th Propulsion Joint Specialist Conference, U. S. Air Force Academy, Colo., June 9–13, 1969; submitted August 11, 1969; revision received July 2, 1970. This work was supported in part by NASA Contract NAS8-19.

* Member of the Technical Staff, Aerothermodynamics Unit, Advanced Projects. Member AIAA.

† Principal Scientist, Heat and Fluid Physics, Research Division. Member AIAA.